COX-2 Inhibitor Celecoxib Suppresses Tumor Growth and Lung Metastasis of a Murine Mammary Cancer

RYOJI YOSHINAKA[1,2], MASA-AKI SHIBATA[1,3], JUNJI MORIMOTO[4], NOBUHIKO TANIGAWA[2] and YOSHINORI OTSUKI[1,3]

[1]Department of Anatomy and Cell Biology, Division of Basic Medicine I, [2]Department of General and Gastroenterological Surgery, Division of Surgery I, [3]High-Tech Research Center, [4]Laboratory Animal Center, Osaka Medical College, Takatsuki, Osaka 569-8686, Japan

Abstract. *Background: The antitumor growth and antimetastatic actions of celecoxib [a selective cyclooxygenase-2 (COX-2) inhibitor] were investigated in a metastatic murine mammary cancer model. Materials and Methods: Mice bearing mammary tumors, developed after inoculation of syngeneic BALB/c mice with a mammary carcinoma cell line carrying a p53 mutation, were treated with celecoxib at 0, 7.5 and 15 mg/kg five times a week for seven weeks. Results: Tumor volumes were significantly reduced in association with an increase in apoptosis and a decrease in DNA synthesis in tumor tissues. In vitro studies demonstrated a significant increase in the number of cells undergoing apoptosis, with significantly elevated activities of caspase-3 and caspase-9, but not caspase-8, and a dose-dependent decrease in mitochondrial membrane potential, indicating the mitochondrial pathway of apoptosis. In addition, treatment with celecoxib showed cell cycle arrest in the G_1-phase and decreased cell population in the S- and G_2/M-phases. Furthermore, tumor microvessel formation and mRNA levels for VEGF-A and COX-2 were markedly decreased. Conclusion: Celecoxib may be useful as an adjuvant therapy for breast cancer containing p53 mutations due to its ability to both induce p53-independent mitochondria-mediated apoptosis and exert anti-angiogenic potential.*

Abbreviations: BrdU, 5-bromo-2'-deoxyuridine; COX, cyclooxygenase; DMSO, dimethyl sulfoxide; H&E, hematoxylin and eosin; LSC, laser scanning cytometer; MMTV, mouse mammary tumor virus; PBS, phosphate-buffered saline; PGE_2, prostaglandin E_2; TUNEL, terminal deoxynucleotidyl transferase-mediated dUTP-FITC nick end-labeling; VEGF-A, vascular endothelial growth factor-A.

Correspondence to: Prof. Yoshinori Otsuki, Department of Anatomy and Cell Biology, Division of Basic Medicine I, Osaka Medical College, 2-7, Daigaku-machi, Takatsuki, Osaka 569-8686, Japan. Tel: +81 72 684 7197, Fax: +81 72 684 6511, e-mail: an1000@art.osaka-med.ac.jp

Key Words: Celecoxib, apoptosis, VEGF, COX-2, angiogenesis, breast cancer.

Two isoforms of cyclooxygenase (COX), the key enzyme catalyzing conversion of arachidonic acid to prostaglandins, have been identified: COX-1 and COX-2. COX-1 is constitutively expressed in most tissues, whereas COX-2 is expressed at sites of inflammation, which has led to the speculation that its inhibition could provide all the benefits of current non-steroidal anti-inflammatory drugs (NSAIDs) without their major side-effects (due to COX-1 inhibition) on the gastrointestinal system (1, 2). The new NSAIDs, which are selective inhibitors of COX-2, can exert therapeutic efficacy without toxic effects due to the inhibition of COX-1. Celecoxib, a selective COX-2 inhibitor, has shown efficacy comparable to that of the NSAIDs on relief of pain and inflammation in osteoarthritis.

Recent studies have indicated that overexpression of COX-2 and prostaglandins is a characteristic of many human cancers, including colorectal, prostate and gastric cancer (3-5). Both breast cancer and breast cancer cell lines (6) exhibit elevated levels of COX-2 that significantly correlate with tumor size and clinical stage (7). In addition, COX-2 inhibition is much more important than COX-1 inhibition in oncogenesis (8, 9). Furthermore, selective COX-2 inhibitors have shown significant effects in reducing the incidence and progression of tumors and metastasis in animal models (7, 8, 10, 11). One example, celecoxib, has been approved for adjuvant treatment of familial adenomatous polyposis and chemoprevention clinical trials of other cancer types (12). The apoptotic and growth inhibitory effects of celecoxib may be mediated through COX-dependent and COX-independent mechanisms (13-15); this versatile agent is capable of targeting multiple sites in signaling pathways regulating cell cycle progression and apoptosis (13, 14, 16).

The lethality of breast cancer is largely the result of metastasis, the most common sites being lung, lymph nodes,

liver and bone. Conventional cancer therapies used in breast cancer have yielded positive results; nevertheless, the rates for cure and survival remain unsatisfactory for a number of reasons, one being the difficulty in controlling and eradicating metastases without serious systemic side effects. Thus, there is a need for the development of more effective and less toxic therapies that can reduce morbidity and mortality. The efficacy of celecoxib for treatment of breast cancer has already been reported, but evaluation of the anti-metastatic ability of celecoxib for mammary cancer remains unsatisfactory. The existence of a mouse metastatic mammary cancer model having a metastatic spectrum similar to that seen in human breast cancers allows further research into these issues. Since one possible action of anticancer agents is against angiogenesis, which has been shown to correlate with a worse prognosis (17), an assessment of vessel numbers and expression of vascular endothelial growth factor-A (VEGF-A), a pro-angiogenesis factor reported to be linked with vascularity, advanced disease and poor prognosis (18, 19) were included in the present study. Recently, celecoxib has been reported to reduce microvessel density in human breast cancer (11), and inhibit VEGF expression in human pancreatic cancer (20).

Materials and Methods

Cells. The BJMC3879 mammary adenocarcinoma cell line used was derived from a metastatic focus within a lymph node from a female BALB/c mouse that had mouse mammary tumor virus (MMTV) injected into the inguinal mammary glands (21). Mammary tumors resulting from MMTV inoculation show a propensity for high metastasis to lungs and lymph nodes (22, 23), a trait retained through culture. BJMC3879 cells are known to feature a p53 mutation (24) and were here maintained in Dulbecco's modified Eagle's medium or RPMI-1640 containing 10% fetal bovine serum with streptomycin/penicillin in an incubator at 37˚C under 5% CO_2.

Animals. A total of 52 female 5-week-old BALB/c mice were used in this study (Japan SLC, Hamamatsu, Japan). The animals were housed four per plastic cage in the preliminary dosage-tolerance study and six per cage in the tumor growth phase, on wood chip bedding, with free access to water and food, under conditions of controlled temperature (21±2˚C), humidity (50±10%) and lighting (12-12 h light-dark cycle). All animals were held for a 2-week acclimatization period before study commencement. All manipulations of mice were performed in accordance with the procedures outlined in the Guide for the Care and Use of Laboratory Animals of Osaka Medical College, Japan.

In vivo preliminary dosage-tolerance study. To ensure that toxicity would not be a factor, a preliminary dosage-tolerance study for the proposed 0 (dimethyl sulfoxide; DMSO), 10, 20 and 30 mg/kg dosages of celecoxib (Wako Pure Chemical Industries, Osaka, Japan) using four mice for each dose was conducted. The animals were injected *i.p.* five times a week for four consecutive weeks. No deaths occurred in any of the groups, and therefore no dose adjustment was considered necessary.

In vivo tumor growth study. BJMC3879 cells [$5x10^6$ cells/0.3 ml phosphate-buffered saline (PBS)] were inoculated *s.c.* into the right inguinal region of 36 female BALB/c mice. Two weeks later, when tumors had grown to ~0.2 cm diameter, groups of 12 mice were injected *i.p.* with 20 μl of either vehicle (100% DMSO) alone or 7.5 or 15 mg/kg celecoxib five times a week for seven weeks. Individual body weights were recorded weekly; using calipers. Each mammary tumor was also measured weekly and tumor volumes calculated using the formula [(maximum diameter) x (minimum diameter)^2 x 0.4] (25). Three hours after the last celecoxib or DMSO treatment all animals were injected *i.p.* with 100 mg/kg 5-bromo-2'-deoxyuridine (BrdU) (Sigma Chemical Co., St. Louis, MO, USA) and 1 h thereafter were killed under diethyl ether anesthesia by exsanguination.

Histopathology. At necropsy, tumors and lymph nodes, routinely those from the axillary and femoral regions and in addition those appearing abnormal, were removed, fixed in 4% formaldehyde solution in phosphate buffer and routinely processed through to paraffin embedding. Lungs were inflated with the formaldehyde solution prior to excision and immersion in fixative. The individual lobes were subsequently removed from the bronchial tree, trimmed into seven pieces and examined for metastatic foci before being similarly processed to paraffin embedding. All paraffin-embedded tissues were cut at 4 μm, with sequential sections stained with hematoxylin and eosin (H&E) for histopathological examination or reserved unstained for immunohistochemistry. For quantitative analysis, lung metastatic foci consisting of >30 cells were counted, as previously described (22).

p53 immunohistochemistry. The avidin-biotin complex method was used for p53 immunohistochemistry. Unstained sections were immersed in distilled water and heated by microwave irradiation for antigen retrieval prior to incubation with an anti-p53 mouse monoclonal antibody (Clone Pab240; Santa Cruz Biotechnology, Santa Cruz, CA, USA) that reacts with the mutant protein in fixed specimens.

DNA synthesis. Tumors from three animals selected from each treatment group were evaluated for DNA synthesis by immunohistochemical demonstration of BrdU incorporation. Using unstained paraffin-embedded tissue sections, DNA was denatured *in situ* by incubation in 4 N HCl solution for 20 min at 37˚C and sections were exposed to an anti-BrdU mouse monoclonal antibody (Clone Bu20a; Dakocytomation, Glostrup, Denmark). The numbers of BrdU-positive S-phase cells per 5,000 cells were counted in (x200) fields of the viable regions in the whole tumor tissue and the BrdU labeling indices were then expressed as the percentages of positive cells of the total counted.

Apoptosis. For quantitative analysis of apoptosis, sections from paraffin-embedded tumors were assayed using the terminal deoxynucleotidyl transferase-mediated dUTP-FITC nick end-labeling (TUNEL) method using an apoptosis *in situ* detection kit (Wako Pure Chemical Industries) with minor modifications to the manufacturer's protocol. Five thousand cells within five randomly selected high power (x200) fields were counted in the viable regions peripheral to necrosis areas and the TUNEL-positive cells expressed as percentages.

In vitro, the BJMC3879 cells, grown in 2-well chamber slides and treated with 20 μM celecoxib for 24 h, were fixed in 4% formaldehyde solution in phosphate buffer and the TUNEL staining procedure was performed, as described above. The numbers of TUNEL-positive

cells per 1,000, counted in four random high power (x400) fields by conventional light microscopy, were expressed as percentages.

Microvessel density in tumors. Immunohistochemical staining using paraffin sections was conducted as in the p53 immunohistochemistry. Unstained sections were incubated with an anti-vWF antibody (Dakocytomation) that reacts with blood endothelial cells. For quantification of tumor microvessel density, vessels in each section were counted in five randomly selected high power (x200) fields of the viable peripheral regions.

Quantitative analysis of VEGF-A and COX-2 expression. Total RNA was isolated from the tumor tissues or the BJMC3879 cells using an RNeasy Mini Kit (Qiagen, GmbH, Hilden, Germany) and cDNAs were synthesized with a Transcriptor First Strand cDNA Synthesis Kit (Roche Diagnostics, GmbH, Mannheim, Germany) following the manufacturer's protocol with the total RNA concentration adjusted to 0.5 μg in each sample. cDNAs were amplified using a LightCycler quick system 330 (Roche Diagnostics) and LightCycler-FastStart DNA Master SYBR Green I (Roche Diagnostics) according to the manufacturer's protocol. Primer sequences were for COX-2, 5'-CAGAAC CGCATT GCCTCTG-3' and 5'- AGCTGTACTCCT GGTCTTCAATGTT-3'; for VEGF-A, 5'-AGG CTG CTG TAA CGA TGA A-3' and 5'-TTT GGT CTG CAT TCA CAT C-3'; and for glyceraldehyde-3-phosphate dehydrogenase (GAPDH), used as an internal control, 5'-TGAACGGGAAGCTCACTGG-3' and 5'-TCCACCACCCTGTTGCTGTA-3' (Nihon Gene Research Lab's Inc., Sendai, Japan). Levels of mRNA were evaluated by a relative quantification method (to each GAPDH mRNA level), as previously described (26).

Cell viability. The BJMC3879 cells were plated 48 h before celecoxib treatment at $1x10^3$ cells/well in 24-well plates. They were subsequently incubated for 24 h with culture medium containing vehicle (DMSO) alone or with medium containing celecoxib at various concentrations up to 40 μM and evaluated for cell proliferation using a Cell Proliferation Kit I (MTT) (Roche Diagnostics).

Cell-cycle distribution. The BJMC3879 cells were grown in 2-well chamber slides (Lab-TekII: Nalgen Nunc International, Naperville, IL, USA), treated with 20 μM celecoxib for 24 h and fixed in cold 70% ethanol. Nuclear DNA was stained with a 50 μg/ml propidium iodide solution containing 100 μg/ml RNase A for 30 min at 37˚C for cell cycle analysis. Cell cycle phases were determined with a microscope-based multiparameter laser scanning cytometer (LSC2; Olympus Optical Co., Tokyo, Japan) and the resulting data analyzed with WinCyte software (Compucyte Co., MA, USA).

Caspase activities. The activities of caspase-8, -9 and -3 were measured in cells treated with 20 μM celecoxib for 24 h using a fluorometric protease assay kit (MBL Inc., Nagoya, Japan), for which cells were lysed with 0.1% Triton X-100 lysis buffer and the protein concentration adjusted to 25 μg in each sample. Caspase activity was measured in terms of fluorescence intensity using a VersaFluor fluorometer (Bio-Rad, Hercules, CA, USA).

Mitochondrial membrane potential ($\Delta\Psi m$). Values for $\Delta\Psi m$ in celecoxib-treated and control cells were measured using a fluorescent cationic dye, 5,5',6,6'-tetrachloro-1,1',3,3'-tetraethylbenzamidazolocarbocyanin iodide (JC-1) (Mit-E-Ψ Mitochondrial Permeability Detection Kit; Biomol Research Laboratories, Plymouth Meeting, PA, USA) 24 h after celecoxib treatment and determined in terms of relative fluorescence units (RFU) using a VersaFluor fluorometer (Bio-Rad) with a 485-495 nm excitation filter and a 585-595 nm emission filter.

Prostaglandin E_2 (PGE_2) levels. Aliquots of $1x10^5$ BJMC3879 cells were plated 48 h before celecoxib treatment in tissue culture flasks (150 cm^2). They were subsequently incubated for 24 h with culture medium containing vehicle (DMSO) alone or with medium containing 20 μM celecoxib. The PGE_2 concentration in 2 ml medium was then assessed by SRL, Inc., Tokyo, Japan.

Statistical analysis. Data for dose-response effects were subjected to analysis of variance (ANOVA), while the Scheffer's *t*-test was employed for assessment of differences between means. Levels of VEGF-A (*in vivo*) were compared using the Least Significant Difference (LSD) method. Data for PGE_2 level, caspase activity, cell cycle parameters, VEGF-A and COX-2 *in vitro* studies were compared between control and celecoxib-treated groups using the two-sided Student's *t*-test. The two-sided Fisher's exact probability test was employed to evaluate the significance of histopathological findings.

Results

Body weights and general condition. The data for body weights of control and celecoxib-treated mice bearing mammary tumors are summarized in Figure 1A. There were no significant differences in body weight among the groups. Single mice in the celecoxib (15 mg/kg)-treated group died at weeks three and four, due to accidents at the time of injection. The general conditions of all other animals remained good throughout the study. This experiment was terminated at experimental week seven when the largest tumor in the control group was 2.0 cm in diameter.

Inhibition of tumor growth and lung metastasis. Tumor volumes are presented in Figure 1B. A significant tumor growth reduction was evident in mice receiving celecoxib in a dose-dependent manner, from week 6 in the 7.5 mg/kg group and week 3 in the 15 mg/kg group. By the end of the experiment, the average tumor volume in control animals was 1462 ± 539 mm^3, while those for mice receiving 7.5 and 15 mg/kg were 804 ± 287 mm^3 and 677 ± 165 mm^3, respectively.

Histopathologically, the mammary carcinomas developed after BJMC3879 cell inoculation proved to be moderately-differentiated adenocarcinomas. Immunohistochemically, they were confirmed to have a p53 mutation (Figure 2A), in agreement with a previous report (24). Lung metastasis occurred in 100% of controls, in 92% of the animals receiving 7.5 mg/kg celecoxib and in 90% of the animals given 15 mg/kg, without significant variation, but the metastatic foci tended to be markedly smaller in both celecoxib-treated groups (Figure 2C) than in the control animals (Figure 2B). Significant decreases in lung metastatic foci consisting of >30 cells were noted in the 7.5 and 15

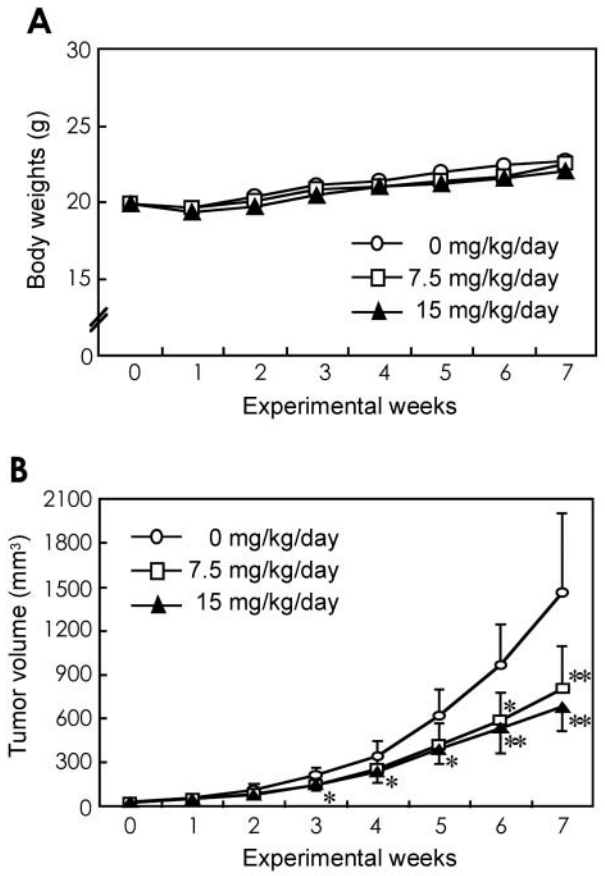

Figure 1. *Body weights (A) and tumor volumes (B) of mice treated with 0 (control), 7.5 or 15 mg/kg celecoxib. Data represent mean±SD. (A) There were no significant differences in body weights among the celecoxib-treated groups compared with the control group. (B) Tumor volume was significantly reduced in mice receiving celecoxib compared to controls (from week 6 in the 7.5 mg/kg mice, and from week 3 in the 15 mg/kg mice) (*p<0.05; **p<0.01).*

mg/kg groups ($p<0.05$ as compared with control) (Figure 3A). The number of metastasis-positive lymph nodes per mouse tended to decrease in a dose-dependent manner, but statistical significance was not attained (Figure 3B).

Levels of DNA synthesis and apoptosis in mammary tumors. DNA synthesis (BrdU-positive S-phase cells) in tumors was significantly decreased in mice receiving celecoxib at 7.5 and 15 mg/kg compared to the controls ($p<0.01$) (Figure 4A). Representative TUNEL-positive cells of tumors in celecoxib-treated and control animals are illustrated in Figures 2D and 2E. The levels of apoptosis in tumors were significantly higher in the 15 mg/kg group ($p<0.01$ as compared to the controls) (Figure 4B).

Microvessel density and relative levels of VEGF-A and COX-2 in mammary carcinomas. Representative tumor microvessels are illustrated in Figures 2F (control) and 2G, a significant decrease being evident in the 7.5 and 15 mg/kg groups compared with the control group (Figure 5A). Relative levels of VEGF-A mRNA were also lower in tumors from the 7.5 and 15 mg/kg groups (Figure 5B). A reduction in the relative levels of COX-2 mRNA was observed in mammary tumors of the 7.5 and 15 mg/kg groups (Figure 5C) but this did not achieve statistical significance due to the large variation in the control tumors.

Cell viability and cell-cycle distribution in vitro. Inhibition of cell growth was seen in celecoxib-treated mammary carcinoma BJMC3879 cells, with significance from 10 μM (Figure 6A). Laser scanning cytometry of the mammary carcinoma cells indicated that celecoxib increased the number of cells in G_1 arrest and suppressed the number entering the S- and G_2/M-phases (Figure 6B).

Apoptosis signaling pathway in vitro. Quantitative analysis revealed a significant increase in the numbers of TUNEL-positive cells after 24 h of 20 μM celecoxib treatment compared with control mammary carcinoma cells (Figure 7A). Significantly elevated activities of caspase-3 and caspase-9, but not caspase-8, were also observed (Figure 7B). The $\Delta\Psi m$ was significantly decreased in celecoxib-treated carcinoma cells compared with control carcinoma cells in a dose-dependent manner (Figure 7C).

VEGF-A and COX-2 expression, and PGE2 levels, in mammary carcinoma cells treated with celecoxib. The relative levels of VEGF-A mRNA were significantly decreased in mammary carcinoma cells treated with 20 μM celecoxib compared with the control cells (Figure 8A). A significant decrease in COX-2 mRNA and PGE_2 was also observed (Figures 8B and C).

Discussion

In this study, the antitumor activity of celecoxib, including suppression of tumor growth and a significant reduction in the number of lung metastases per mouse, was associated with inhibition of angiogenesis, determined by evaluating tumor microvessel formation. Furthermore, this was associated with decreased levels of VEGF-A mRNA *in vivo* and *in vitro* as assessed using real-time RT-PCR. The results, thus, suggest that suppression of tumor growth and metastasis by celecoxib may be directly related to depressed VEGF-A expression and anti-angiogenesis.

Breast cancer is one of the leading causes of cancer mortality in women throughout the world, including Japan, but tumors confined within the breast can be surgically removed with a good prognosis. However, mean survival for patients with metastases to the lymph nodes, bone, lungs, liver and/or brain is only 18 to 24 months and responses to

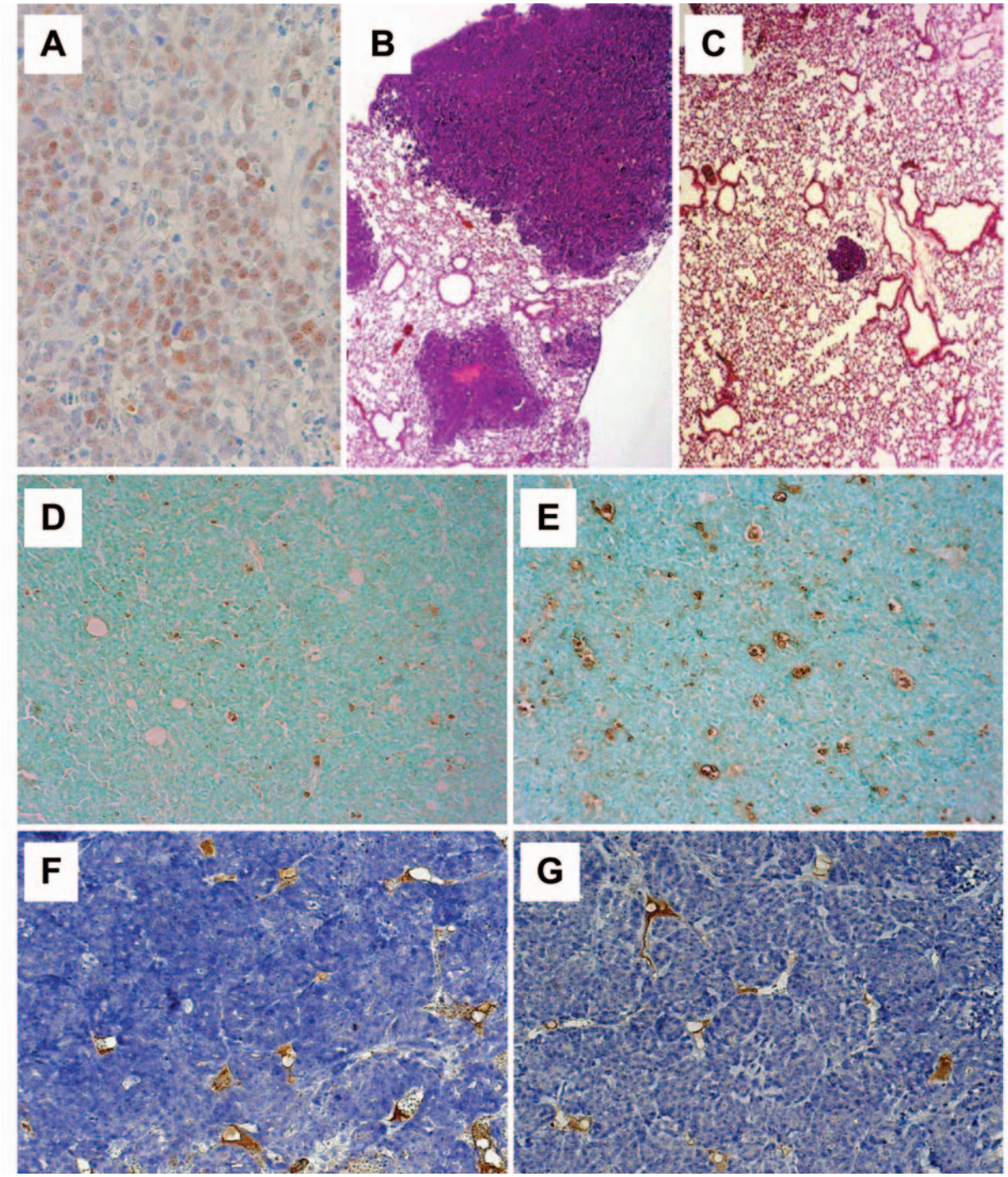

Figure 2. *(A) p53 immunohistochemistry in a BJMC3879 mammary carcinoma. Note nuclear staining of abnormal p53 protein. p53 immunohistochemistry, x400. (B) Lung metastatic nodules from a control mouse treated with DMSO alone. (C) Lung metastatic foci from a mouse treated with 15 mg/kg celecoxib. Note the difference in size between (B) and (C), H&E, x40. TUNEL-positive (apoptotic) cells in mammary carcinomas after treatment with 15 mg/kg celecoxib (E) and in a vehicle control (D). (D) and (E), TUNEL, x200. Tumor microvessel densities in mammary carcinomas after treatment with 15 mg/kg celecoxib (G) and in a vehicle control (F). (F) and (G), vWF immunohistochemistry, x200.*

chemotherapy or endocrine therapy are limited to ~50% (27). Clearly, there is a need for the development of novel therapies to complement the existing triad of surgery, radiation and chemotherapy. Breast and other tumors often have increased levels of prostaglandins, particularly PGE (28), which is also associated with metastasis to bone and poor

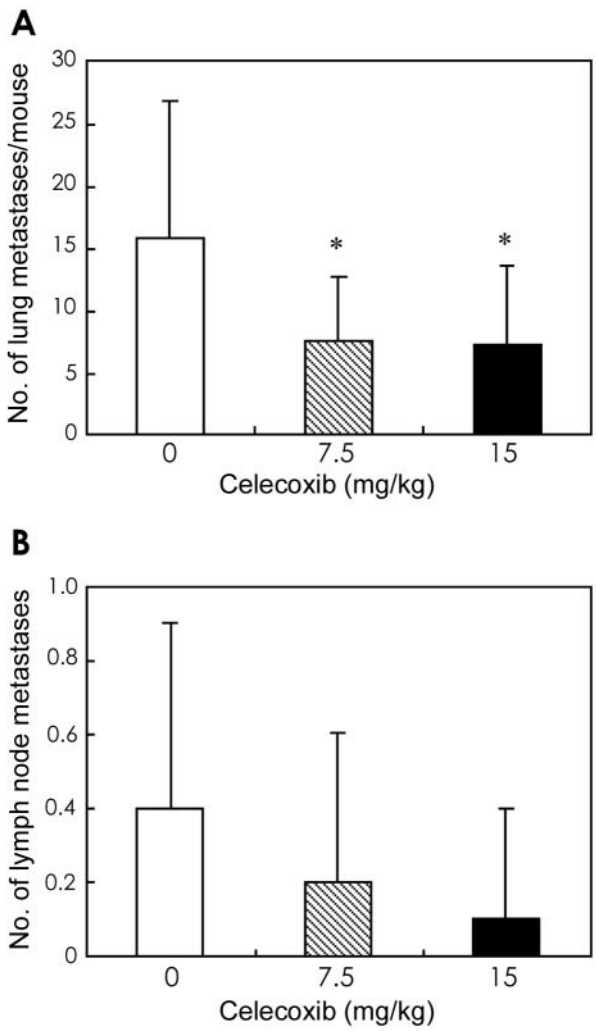

Figure 3. *(A) Lung metastases were categorized as microscopic foci composed of >30 cells. In the 7.5 and 15 mg/kg groups, numbers of foci per mouse were significantly reduced (*p<0.05). (B) The number of metastasis-positive lymph nodes per mouse tended to decrease in a dose-dependent manner, but without statistical significance. Data represent mean±SD.*

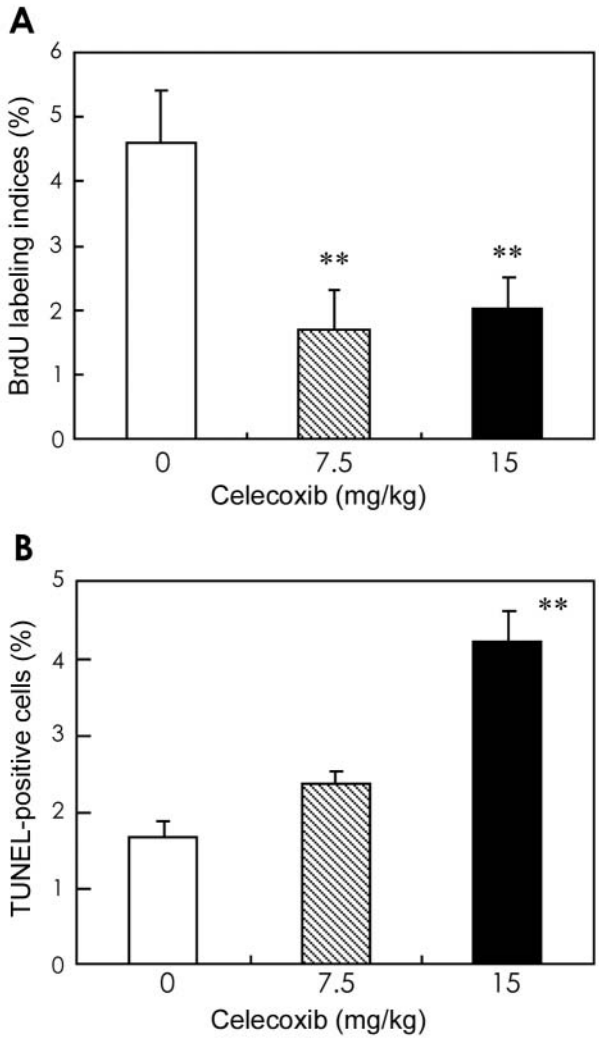

Figure 4. *(A) DNA synthesis in tumors, assessed by BrdU labeling indices, was significantly decreased in mice receiving celecoxib at 7.5 and 15 mg/kg (**p<0.01). (B) Levels of apoptosis, evaluated by TUNEL assay, were significantly higher in the 15 mg/kg group compared with tumors from the control mice (**p<0.01).*

survival (29, 30). Our present finding that PGE_2 levels were significantly decreased in mammary carcinoma cells treated with celecoxib is, therefore, of interest. The main inducible enzyme responsible for its production, COX-2, is commonly overexpressed in both rodent and human tumors (7). Since the risk of developing cancer may be attributable to the combined actions of environmental factors and endogenous promoting agents (31, 32), identification of the latter may lead not only to a better understanding of the processes of tumor progression and metastasis, but may also provide new strategies for developing chemopreventive agents. Administration of selective COX-2 inhibitors in humans may reduce the risk of cancer development (33) and our present results point to their efficacy against breast cancer.

Celecoxib is known to induce apoptosis (13, 14), with two pathways currently being thought to play major roles in the regulation of this type of mammalian cell death: an extrinsic pathway mediated by one or more death receptors involving caspase-8 and -3, and an intrinsic pathway mediated by mitochondria involving caspase-9 and -3 (34, 35). Here, it has been confirmed that celecoxib-induced cell death involved apoptosis rather than necrosis using the TUNEL assay. In addition, significantly elevated activities of caspase-3 and caspase-9, but not caspase-8, were observed in the BJMC3879 cells treated with celecoxib, strongly suggesting activation of the intrinsic mitochondrial pathway. This was further indicated by the significant decrease in $\Delta\Psi m$ apparent in the celecoxib-treated cells. Since 50% of human

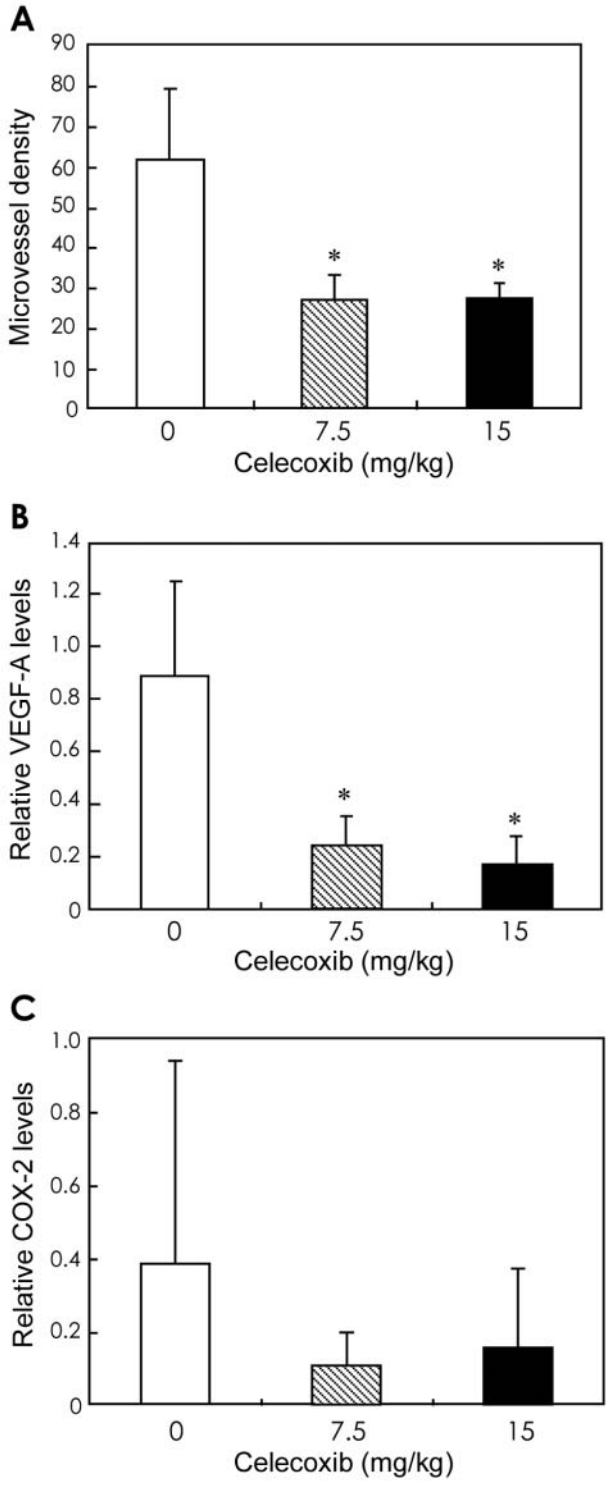

Figure 5. *(A) Microvessel densities were significantly decreased in tumors from the 7.5 and 15 mg/kg groups compared with tumors from the control mice (*p<0.05). (B) Relative levels of VEGF-A mRNA, assessed by real-time PCR, were significantly lower in the 7.5 and 15 mg/kg groups (*p<0.05). (C) Relative levels of COX-2 mRNA tended to be lower in the 7.5 and 15 mg/kg groups but without statistical significance because of the large variation in the control group. Data represent mean±SD.*

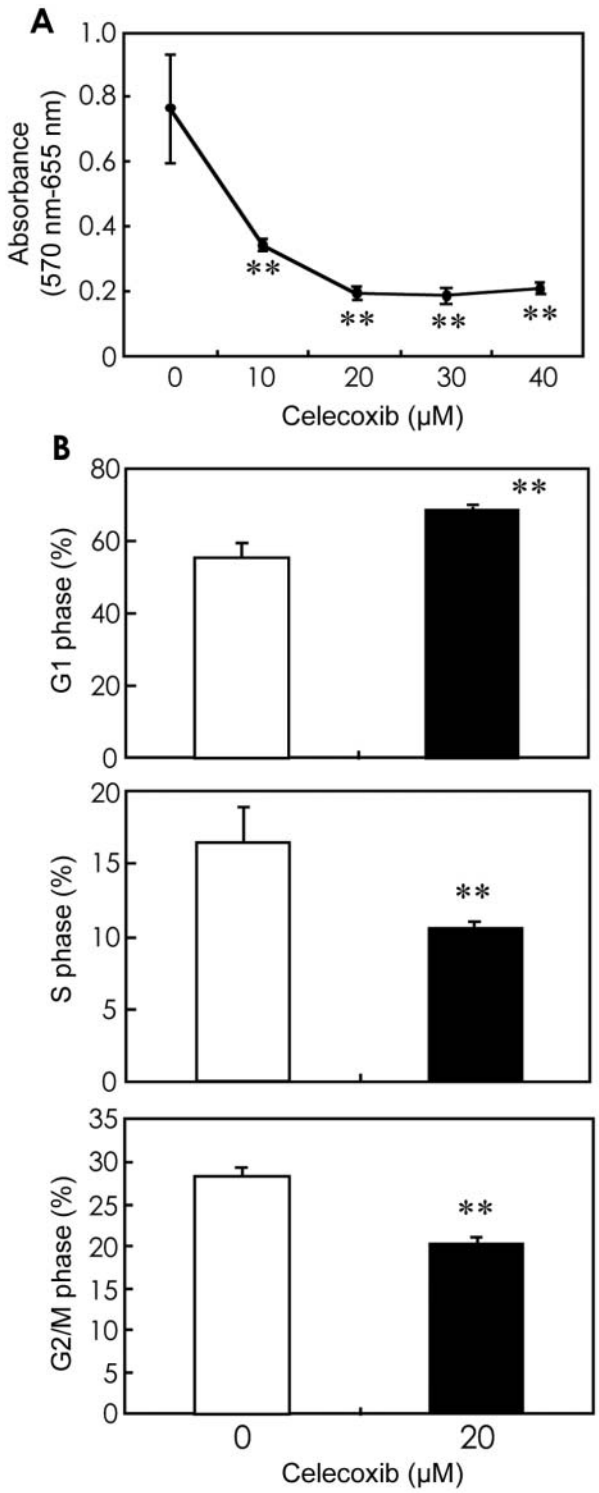

Figure 6. *(A) Dosage determination for mouse mammary carcinoma-derived BJMC3879 cells with 0, 10, 20, 30 or 40 μM celecoxib. Inhibition of cell growth was seen in celecoxib-treated cells (**p<0.01). (B) Cell-cycle distribution (percentage of cells in a specified phase) after treatment of mammary carcinoma cells with 20 μM celecoxib. Note the arrest in G_1-phase and reduction of cells in both the S- and G_2/M-phases (**p<0.01). Data represent mean±SD.*

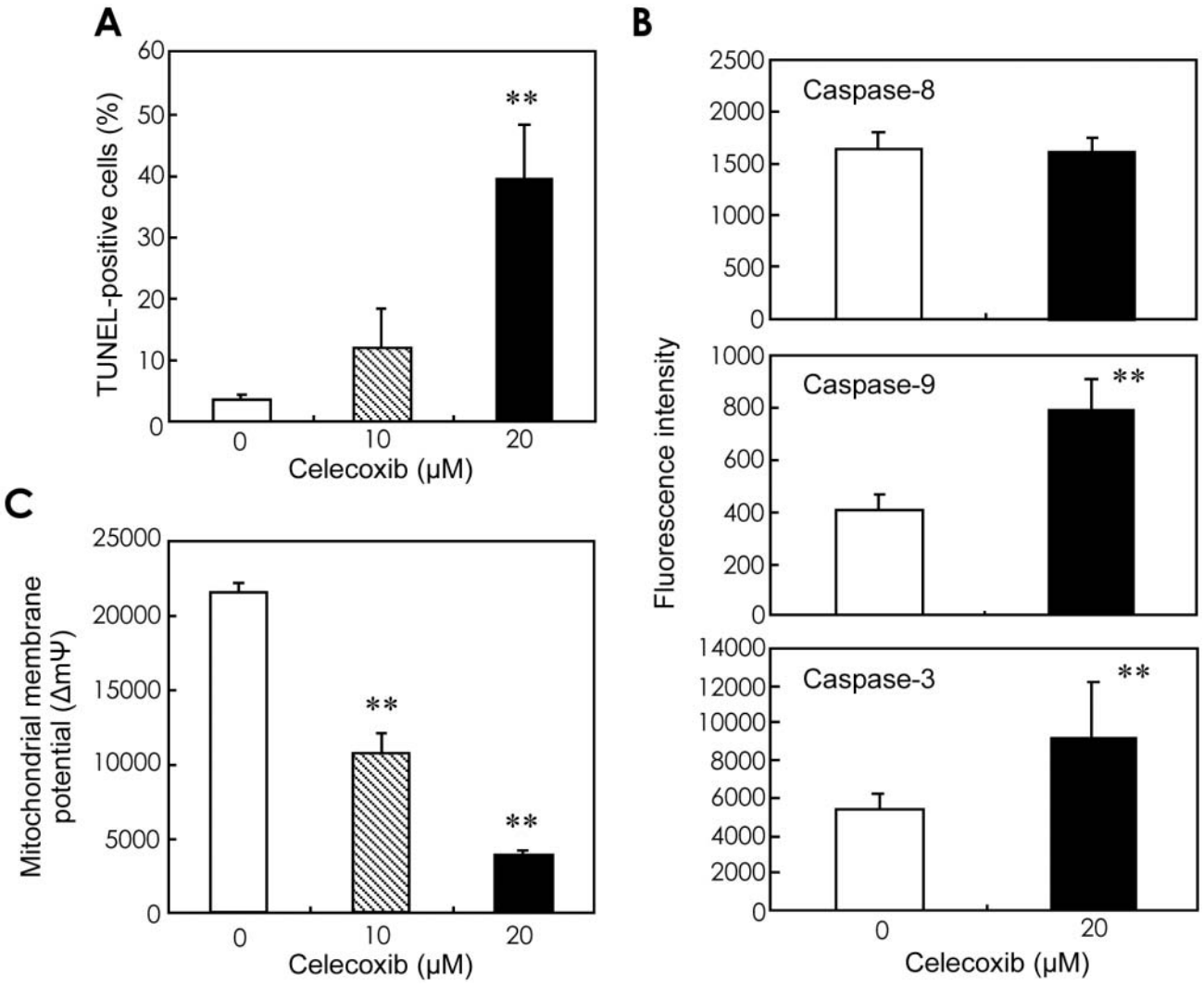

Figure 7. *Mammary carcinoma BJMC3879 cells, with or without celecoxib treatment for 24 h, were analyzed for apoptosis using the TUNEL assay. (A) The numbers of TUNEL-positive (apoptotic) cells were significantly increased in a dose-dependent manner with 20 μM celecoxib treatment (**p<0.01). Four samples of both control using fluorometric assays. Note significant elevation of activities of caspase-3 (*p<0.05) and caspase-9 (**p<0.01) in the BJMC3879 cells treated with 20 μM celecoxib for 24 h, but no significant effects on caspase-8 activity. (C) Mitochondrial membrane potential (ΔΨm) measured with a fluorescent cationic dye JC-1. Celecoxib induced a significant decrease in ΔΨm in a dose-dependent manner (**p<0.01). Data represent mean±SD.*

cancers have mutations in *p53* (36), like the present cell line (24), the fact that celecoxib induces a *p53*-independent apoptotic response may be highly relevant to treating human neoplasms. Our laser scanning cytometric analysis *in vitro* demonstrated that celecoxib inhibited DNA synthesis and cell growth with arrest at G_1 and reduced transition to the S- and G_2/M-phases of the cell cycle, in line with the significant decrease in BrdU-positive S-phase cells. In fact, it has been shown that celecoxib increases expression of $p21^{Waf1}$ and $p27^{Kip1}$ (16) which might be related to up-regulation of these cell cycle inhibitory proteins.

Angiogenesis, the process of new blood vessel formation, is considered critical for the growth of tumors and has been shown to correlate with a poor prognosis (17). It was previously reported that COX-2 is expressed in most cancer tissues including those of the breast, and the presence of COX-2 is associated with angiogenic vasculature in most tumors (37). Furthermore, celecoxib blocks angiogenesis and suppresses implanted human colon carcinoma cells in nude mice (37). Recently, there have been reports that PGE_2 induces angiogenesis (38), and celecoxib has been shown to reduce microvessel density in human breast cancer (11). Thus, the present results can be viewed as providing support for the hypothesis of a link between apoptosis and inhibited cell proliferation, on the one hand, and angiogenesis on the other, through actions on COX-2 and PGE_2. More recently, it has

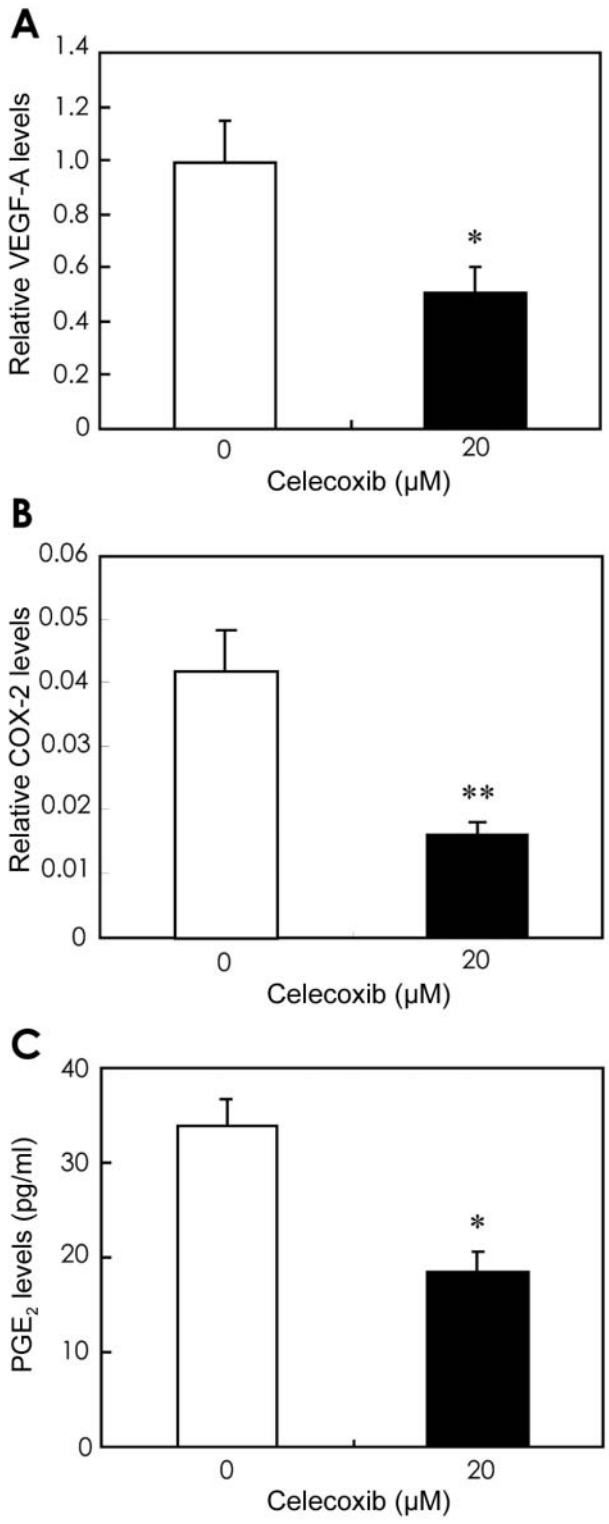

Figure 8. *Relative levels of VEGF-A (A) and COX-2 (B) mRNAs, measured by real-time RT-PCR, were significantly lower in mammary carcinoma cells treated with 20 μM celecoxib compared to the control levels (*p<0.05; **p<0.01). (C) PGE_2 levels were also significantly lower in mammary carcinoma cells treated with 20 μM celecoxib compared with control cells (*p<0.05). Data represent mean±SD.*

been demonstrated that celecoxib can inhibit angiogenesis *via* inhibition of VEGF expression by reduction of the Sp1 promoter (20). In addition, celecoxib may act on the HIF-1α pathway. In the present study, although celecoxib at 7.5 and 15 mg/kg significantly reduced metastasis, BrdU labeling indices, microvessel density and VEGF-A levels, a clear dose-response was lacking and the inhibitory effects were similar between the 7.5 and 15 mg/kg groups. The 7.5 mg/kg dosage may show maximum effects and celecoxib at 15 mg/kg may induce some pharmacological toxicity, albeit without reduction in body weight. In fact, COX-2 levels in tumors showed the lowest levels in the 7.5 mg/kg group. It has been reported that once breast cancers reach ≥4 cm, the chances of tumor recurrence or metastasis increase dramatically (39). Thus, celecoxib-inhibition of tumor growth *via* inducing apoptosis, inhibiting DNA synthesis and reducing angiogenesis may be useful for chemoprevention and adjuvant therapy.

Acknowledgements

This investigation was supported by a High-Tech Research Center grant at Osaka Medical College from the Ministry of Education, Culture, Sports, Science and Technology of Japan.

References

1 Zhang F, Warskulat U, Wettstein M, Schreiber R, Henninger HP, Decker K and Haussinger D: Hyperosmolarity stimulates prostaglandin synthesis and cyclooxygenase-2 expression in activated rat liver macrophages. Biochem J *312(Pt 1)*: 135-143, 1995.

2 Feng L, Xia Y, Yoshimura T and Wilson CB: Modulation of neutrophil influx in glomerulonephritis in the rat with anti-macrophage inflammatory protein-2 (MIP-2) antibody. J Clin Invest *95*: 1009-1017, 1995.

3 Sano H, Kawahito Y, Wilder RL, Hashiramoto A, Mukai S, Asai K, Kimura S, Kato H, Kondo M and Hla T: Expression of cyclooxygenase-1 and -2 in human colorectal cancer. Cancer Res *55*: 3785-3789, 1995.

4 Ristimaki A, Honkanen N, Jankala H, Sipponen P and Harkonen M: Expression of cyclooxygenase-2 in human gastric carcinoma. Cancer Res *57*: 1276-1280, 1997.

5 Yoshimura R, Sano H, Masuda C, Kawamura M, Tsubouchi Y, Chargui J, Yoshimura N, Hla T and Wada S: Expression of cyclooxygenase-2 in prostate carcinoma. Cancer *89*: 589-596, 2000.

6 Subbaramaiah K, Telang N, Ramonetti JT, Araki R, DeVito B, Weksler BB and Dannenberg AJ: Transcription of cyclooxygenase-2 is enhanced in transformed mammary epithelial cells. Cancer Res *56*: 4424-4429, 1996.

7 Taketo MM: Cyclooxygenase-2 inhibitors in tumorigenesis (Part II). J Natl Cancer Inst *90*: 1609-1620, 1998.

8 Oshima M, Dinchuk JE, Kargman SL, Oshima H, Hancock B, Kwong E, Trzaskos JM, Evans JF and Taketo MM: Suppression of intestinal polyposis in Apc delta716 knockout mice by inhibition of cyclooxygenase 2 (COX-2). Cell *87*: 803-809, 1996.

9 Reddy BS, Rao CV and Seibert K: Evaluation of cyclooxygenase-2 inhibitor for potential chemopreventive properties in colon carcinogenesis. Cancer Res *56*: 4566-4569, 1996.

10 Basu GD, Pathangey LB, Tinder TL, Lagioia M, Gendler SJ and Mukherjee P: Cyclooxygenase-2 inhibitor induces apoptosis in breast cancer cells in an *in vivo* model of spontaneous metastatic breast cancer. Mol Cancer Res *2*: 632-642, 2004.

11 Zhang S, Lawson KA, Simmons-Menchaca M, Sun L, Sanders BG and Kline K: Vitamin E analog alpha-TEA and celecoxib alone and together reduce human MDA-MB-435-FL-GFP breast cancer burden and metastasis in nude mice. Breast Cancer Res Treat *87*: 111-121, 2004.

12 Steinbach G, Lynch PM, Phillips RK, Wallace MH, Hawk E, Gordon GB, Wakabayashi N, Saunders B, Shen Y, Fujimura T, Su LK and Levin B: The effect of celecoxib, a cyclooxygenase-2 inhibitor, in familial adenomatous polyposis. N Engl J Med *342*: 1946-1952, 2000.

13 Ding H, Han C, Zhu J, Chen CS and D'Ambrosio SM: Celecoxib derivatives induce apoptosis *via* the disruption of mitochondrial membrane potential and activation of caspase 9. Int J Cancer *113*: 803-810, 2005.

14 Jendrossek V, Handrick R and Belka C: Celecoxib activates a novel mitochondrial apoptosis signaling pathway. Faseb J *17*: 1547-1549, 2003.

15 Tegeder I, Pfeilschifter J and Geisslinger G: Cyclooxygenase-independent actions of cyclooxygenase inhibitors. Faseb J *15*: 2057-2072, 2001.

16 Grosch S, Tegeder I, Niederberger E, Brautigam L and Geisslinger G: COX-2 independent induction of cell cycle arrest and apoptosis in colon cancer cells by the selective COX-2 inhibitor celecoxib. Faseb J *15*: 2742-2744, 2001.

17 Takebayashi Y, Akiyama S, Yamada K, Akiba S and Aikou T: Angiogenesis as an unfavorable prognostic factor in human colorectal carcinoma. Cancer *78*: 226-231, 1996.

18 Takahashi Y, Kitadai Y, Bucana CD, Cleary KR and Ellis LM: Expression of vascular endothelial growth factor and its receptor, KDR, correlates with vascularity, metastasis, and proliferation of human colon cancer. Cancer Res *55*: 3964-3968, 1995.

19 Takahashi Y, Tucker SL, Kitadai Y, Koura AN, Bucana CD, Cleary KR and Ellis LM: Vessel counts and expression of vascular endothelial growth factor as prognostic factors in node-negative colon cancer. Arch Surg *132*: 541-546, 1997.

20 Wei D, Wang L, He Y, Xiong HQ, Abbruzzese JL and Xie K: Celecoxib inhibits vascular endothelial growth factor expression in and reduces angiogenesis and metastasis of human pancreatic cancer *via* suppression of Sp1 transcription factor activity. Cancer Res *64*: 2030-2038, 2004.

21 Morimoto J, Imai S, Haga S, Iwai Y, Iwai M, Hiroishi S, Miyashita N, Moriwaki K and Hosick HL: New murine mammary tumor cell lines. In Vitro Cell Dev Biol *27A*: 349-351, 1991.

22 Shibata MA, Morimoto J and Otsuki Y: Suppression of murine mammary carcinoma growth and metastasis by HSVtk/GCV gene therapy using *in vivo* electroporation. Cancer Gene Ther *9*: 16-27, 2002.

23 Shibata MA, Ito Y, Morimoto J, Kusakabe K, Yoshinaka R and Otsuki Y: *In vivo* electrogene transfer of interleukin-12 inhibits tumor growth and lymph node and lung metastases in mouse mammary carcinomas. J Gene Med *8*: 335-352, 2006.

24 Shibata MA, Ito Y, Morimoto J and Otsuki Y: Lovastatin inhibits tumor growth and lung metastasis in mouse mammary carcinoma model: a p53-independent mitochondrial-mediated apoptotic mechanism. Carcinogenesis *25*: 1887-1898, 2004.

25 Shibata MA, Liu ML, Knudson MC, Shibata E, Yoshidome K, Bandey T, Korsmeyer SJ and Green JE: Haploid loss of bax leads to accelerated mammary tumor development in C3(1)/SV40-TAg transgenic mice: reduction in protective apoptotic response at the preneoplastic stage. Embo J *18*: 2692-2701, 1999.

26 Livak KJ and Schmittgen TD: Analysis of relative gene expression data using real-time quantitative PCR and the 2(-Delta Delta C(T)) method. Methods *25*: 402-408, 2001.

27 Ellis MJ, Hayes DF and Lippman ME: Treatment of metastatic breast cancer. *In*: Disease of the Breast. Haris JR, Lippman ME, Morrow M, Osborne CK (eds.). PA, USA: Lippincott Williams & Wilkins, pp. 749-797, 2000.

28 Karmali RA, Welt S, Thaler HT and Lefevre F: Prostaglandins in breast cancer: relationship to disease stage and hormone status. Br J Cancer *48*: 689-696, 1983.

29 Bennett A, Charlier EM, McDonald AM, Simpson JS, Stamford IF and Zebro T: Prostaglandins and breast cancer. Lancet *2*: 624-626, 1977.

30 Bennett A, Berstock DA, Raja B and Stamford IF: Survival time after surgery is inversely related to the amounts of prostaglandins extracted from human breast cancers. Br J Pharmacol *66*: 451P, 1979.

31 Potter JD: Risk factors for colon neoplasia – epidemiology and biology. Eur J Cancer *31A*: 1033-1038, 1995.

32 Giovannucci E and Willett WC: Dietary factors and risk of colon cancer. Ann Med *26*: 443-452, 1994.

33 Thun MJ, Namboodiri MM, Calle EE, Flanders WD and Heath CW Jr: Aspirin use and risk of fatal cancer. Cancer Res *53*: 1322-1327, 1993.

34 Hengartner MO: The biochemistry of apoptosis. Nature *407*: 770-776, 2000.

35 Otsuki Y: Tissue specificity of apoptotic signal transduction. Med Electron Microsc *37*: 163-169, 2004.

36 Greenblatt MS, Bennett WP, Hollstein M and Harris CC: Mutations in the p53 tumor suppressor gene: clues to cancer etiology and molecular pathogenesis. Cancer Res *54*: 4855-4878, 1994.

37 Masferrer JL, Leahy KM, Koki AT, Zweifel BS, Settle SL, Woerner BM, Edwards DA, Flickinger AG, Moore RJ and Seibert K: Antiangiogenic and antitumor activities of cyclooxygenase-2 inhibitors. Cancer Res *60*: 1306-1311, 2000.

38 Chang SH, Liu CH, Conway R, Han DK, Nithipatikom K, Trifan OC, Lane TF and Hla T: Role of prostaglandin E2-dependent angiogenic switch in cyclooxygenase 2-induced breast cancer progression. Proc Natl Acad Sci USA *101*: 591-596, 2004.

39 Carter CL, Allen C and Henson DE: Relation of tumor size, lymph node status, and survival in 24,740 breast cancer cases. Cancer *63*: 181-187, 1989.

Received July 31, 2006
Accepted October 18, 2006